Numerical Finite Difference Techniques for the Investigation of Critical Behaviour in the Spherically Symmetric Collapse of SU(2) Yang-Mills Fields

Tyler Dodds*

Department of Physics and Astronomy, University of British Columbia
6224 Agricultural Road, Vancouver, British Columbia, Canada, V6T 1Z1
(Dated: November 14, 2006)

Finite difference numerical methods will be used to investigate critical phenomena in spherically symmetric gravitational collapse of an abelian gauge, magnetic ansatz SU(2) Yang-Mills field and a massless scalar field minimally coupled to gravity. We wish to confirm the existence and universality of *critical solutions* for different families of initial data, which exhibit time-repeating spatial structure, and the power-law mass scaling of black holes. With an appropriate choice of coordinates, the geometry is specified by only two functions; these are to be solved for, along with the equations of motion of each field. The resultant coupled partial differential equations will be solved by use of finite difference approximations, employing techniques such as adaptive mesh refinement as necessary for computational efficiency.

I. MOTIVATION

A generic, isolated system acting under general relativity evolves on a long time scale based on the competition between the dispersive effects of the kinetic energy of the system and its gravitational self-attraction. With minimal gravitational interaction, a system will tend to disperse to infinity. Systems with strong gravitational self-interaction will tend to collapse, forming a black hole. A binary system of two black holes orbiting each other, for example, will also collapse into a single black hole, due to emission of gravitational waves [16].

Historically, the model problem for critical collapse consisted of a massless scalar field in spherical symmetry. A massless scalar field corresponds to radiation propagating at the speed of light. The dynamics of the solution depend greatly on the initial radial distribution of the scalar field, with large qualitative differences between weak and strong (roughly, low and high energy density, respectively) initial data. With sufficiently weak initial data, the system disperses, and evolves into an increasingly flat spacetime [10]. However, with sufficiently strong initial data, the system collapses into a black hole, with very little radiation dispersing to infinity [11]. The phenomenon of *critical behaviour* in gravitational collapse was found through investigation of initial data with energy densities between the aforementioned limits. There are three principle features of critical behaviour, hereafter described.

Critical behaviour arises from consideration a family of initial data parameterized by p. For example, the initial data could be a Gaussian distribution, while the parameter p could be the amplitude or width of the distribution. In general, p is chosen to scale with the energy density or strength of gravitational self-interaction of the field, so smaller p limit to weak initial data, and larger p limit to

strong initial data with the behaviour discussed above. The hallmark of critical behaviour is the existence of a it critical parameter value p^* that bisects the range of p, with black holes forming for $p > p^*$ [6].

The first feature of critical behaviour is *universality*. This means that the behaviour of the critical solution for $p = p^*$ is unique, up to rescaling of units, across different families of initial data. Figure 1 shows the universality of a near-critical solution with a massless scalar field as the matter source. Each of the four solutions evolve with identical profiles over time, despite being given different families of initial conditions.
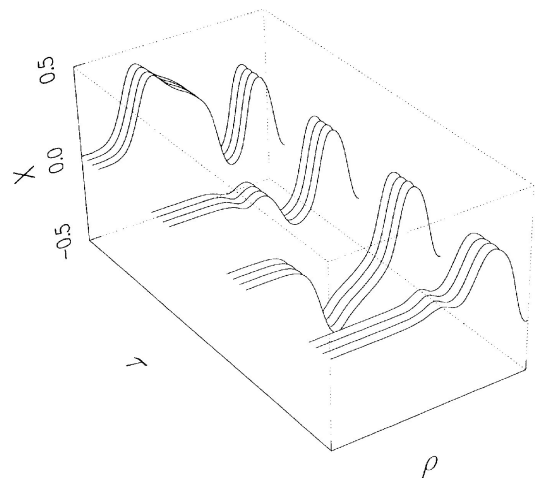

FIG. 1: Universality of a near-critical solution of a massless scalar field. At each time coordinate τ is a group of four different solutions of a massless scalar field. Each profile has a different family of initial data, with scaling chosen for each family to maximize agreement at the earliest τ. The consistent evolution shows the universality of the critical solution, independent of its initial form.

The second feature of critical behaviour is called *scale echoing*. The critical solution $\phi_{\mathrm{crit}}(r, t)$ is invariant under

a certain scaling of both space and time, namely

$$\phi_{\text{crit}}(r, t - t^*) = \phi_{\text{crit}}(e^{\Delta} r, e^{\Delta}(t - t^*)), \qquad (1)$$

for $t < t^*$, with t^* the time after which all scale echoing is completed. Here Δ is a dimensionless parameter that is, like the critical solution itself, family-independent. Figure 2 shows this behaviour for a near-critical solution of a massless scalar field, where the profile is identical to one at a time e^{Δ} closer to t^*, but on a spatial scale e^{Δ} smaller.
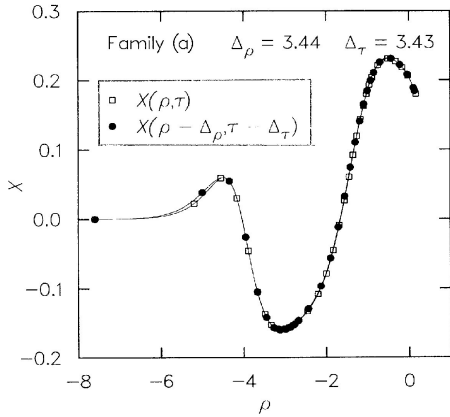

FIG. 2: Scale echoing property of a near-critical solution of a massless scalar field. The curve marked with solid circles is on a spatial scale $e^{\Delta_\rho} \approx 30$ times smaller than the curve marked by open squares, but is at a time $e^{\Delta_\tau} \cong e^{\Delta_\rho}$ closer to the time when the 'echoing' behaviour ceases. The two profiles agree under this specific scaling.

The third and perhaps most interesting feature of critical behaviour is the scaling of the black hole mass with the parameter p. In the region $p > p^*$, where black holes form, it is found that the mass of the black hole, M_{BH}, varies as

$$M_{\text{BH}} = c_f |p - p^*|^{\gamma}. \qquad (2)$$

Here, γ is a *second* family-independent dimensionless parameter; only the scaling factor c_f depends on the family of initial data. This is referred to as type II critical phenomena, where black holes of arbitrarily small mass can be created. Figure 3 shows the mass scaling relationship in type II black hole formation for a massless scalar field. The identical slopes seen for all three types of initial data indicates the same power law growth of the black hole mass with parameter p, regardless of the form of the initial data.

There is also a classification of type I critical behaviour, characterized by the creation of a minimum mass black hole at the critical value of the parameter p^*. Instead the lifetime of the solution, τ_0, the length of time that it corresponds to the critical solution, obeys the scaling relationship

$$\tau_0 = d_f |p - p^*|^{\sigma}. \qquad (3)$$

As usual, σ is family independent. In type I behaviour, the near-characteristic solutions are invariant under time translations rather than time and space rescaling; thus, they are either static or period. This behaviour has been observed, for example, in the collapse of a massive scalar field [4].
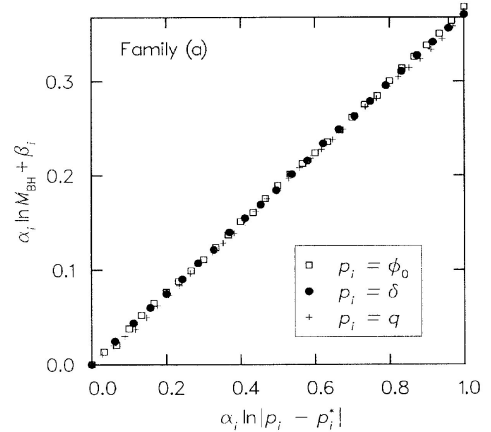

FIG. 3: Black hole mass scaling in type II gravitational collapse of a massless scalar field. The black hole mass variation with the difference of the initial data parameter p from the critical value p^* is plotted on a log-log scale. Each of the three markers corresponds to a different type of initial data. Each family of markers is plotted so as to normalize the domain and place the smallest-mass black hole at the origin.

As with the proposed research, much of the investigation of critical phenomena has been done in spherical symmetry. However, critical behaviour is not merely an accident of the dynamics of a spherically symmetric massless scalar field. Critical behaviour of the massless scalar field has been documented in four and five spatial dimensions [12]. Most investigations, however, assume a matter content different from a massless scalar field. Among these are massive scalar fields, scalar fields coupled to electromagnetism, perfect fluids, and Yang-Mills fields, all of which generate critical behaviour. The few investigations in axial symmetry suggest that critical behaviour is more general than spherical symmetry [1, 8].

In this investigation we focus on the critical behaviour of Yang-Mills fields – in particular, an abelian gauge, magnetic ansatz SU(2) field – along with a massless scalar field, minimally coupled to gravity. This is a simple model that will be used to explore the possible dynamics and phenomena that can arise in the collapse of a non-abelian gauge field. Gauge theories enforce not only global symmetries under certain transformation, but also ask for symmetries to hold locally as well. The SU(2) Yang-Mills field is a canonical example of a field in such a theory, while the abelian gauge magnetic ansatz is a further simplification, made to capture the essential dynamics while keeping the system easy to describe.

II. THEORY

Most numerical work in relativity decomposes the spacetime into the temporal dimension and spatial dimensions. The most often used formalism is called the 3+1 ADM formalism, first seen from Arnowitt, Deser and Misner [2]. This views the spacetime as a family of three-dimensional spacelike hypersurfaces. Since ordinary matter moves along timelike curves, its trajectory will be given by a unique position along each hypersurface. This formalism will generate the spacetime and matter field as an initial value problem, once a particular initial hypersurface is completely characterized.

In relativity, the metric provides infinitesimal distances between neighbouring points in spacetime, thus describing its geometry. The most general time-dependent metric under spherical symmetry can be written [14] as

$$ds^2 = (-\alpha^2 + a^2\beta^2)dt^2 + 2a^2\beta dt dr + a^2 dr^2 + r^2 b^2 d\Omega^2, \quad (4)$$

with α, β, a and b functions of r and t, and

$$d\Omega^2 = d\theta^2 + \sin^2\theta d\varphi^2. \quad (5)$$

Here, θ and φ comprise the usual set of angles in spherical coordinates. It is convenient to adopt polar and areal coordinates, with $\beta = 0$ and $b = 1$ [3]. This simplifies the metric to

$$ds^2 = -\alpha^2 dt^2 + a^2 dr^2 + r^2 d\Omega^2. \quad (6)$$

This makes the hypersurfaces of the 3+1 formalism normal to the t coordinate. Furthermore, the coordinate r provides a measure of the proper surface area in this case, with $A = 4\pi r^2$.

Under the imposition of spherical symmetry, the choice of metric (6), and the particular assumptions regarding the SU(2) field (namely, abelian gauge and magnetic ansatz), it happens that one can view the matter content as a single function $W(r,t)$, which acts analogous to a potential [7]. There is an associated Lagrangian scalar

$$L_M = -\left(\frac{g^{\mu\nu}\nabla_\mu W \nabla_\nu W}{r^2} + \frac{1}{2}\frac{(1-W^2)^2}{r^4}\right). \quad (7)$$

The by the principle of minimal coupling, one can picture the system as being given by a total Lagrangian which is the sum of the free gravitational Lagrangian $\mathcal{L}_g$ and the matter Lagrangian $\mathcal{L}_M$,

$$\mathscr{L} = \mathcal{L}_g + \mathcal{L}_M = \sqrt{-g}\,(R + L_M), \quad (8)$$

with R the Ricci scalar, and g the determinant of the metric (6). In minimally coupling another field – like the proposed massless scalar field – to the system, one would add a Lagrangian scalar $\mathcal{L}_\phi$ to (8) that describes the new field.

The Einstein equations governing the geometric variables (metric coefficients) a and α are recovered by extremizing the action with respect to variations in a and α, after suitable definition of the stress-energy tensor $T_{\mu\nu}$ that satisfies local conservation. The equations of motion are given by extremizing the action with respect to variations in the specific field [5]. Since minimal coupling as in (8) is linear, extremizing the action with respect to variations in a specific field will yield the same equations of motion regardless of any other couplings to the system. Each field evolves solely due to the geometry of the spacetime and its equation of motion; the geometry itself evolves based on the matter content – namely, the fields that have been coupled.

Solving the equations of motion for the system given by the Lagrangian (8) can be reduced to solving a system of partial differential equations for the metric coefficients and the derivatives of the Yang-Mills potential:

$$\Phi_t = \left(\frac{\alpha}{a}\Pi\right)_r, \quad (9)$$

$$\Pi_t = \left(\frac{\alpha}{a}\Phi\right)_r + \frac{a\alpha}{r^2}W(1-W^2), \quad (10)$$

$$0 = \frac{a_r}{a} + \frac{a^2-1}{r^2} \quad (11)$$
$$-\frac{1}{r}\left(\Phi^2 + \Pi^2 + \frac{a^2}{2r^2}(1-W^2)^2\right),$$

$$0 = \frac{\alpha_r}{\alpha} - \frac{a^2-1}{r^2} \quad (12)$$
$$-\frac{1}{r}\left(\Phi^2 + \Pi^2 - \frac{a^2}{2r^2}(1-W^2)^2\right),$$

where

$$\Phi = W_r, \quad (13)$$
$$\Pi = \frac{a}{\alpha}W_t, \quad (14)$$

so that

$$W(r,t) = W_0 + \int_0^r \Phi(x,t)dx \quad (15)$$

describes the Yang-Mills field.

These equations are subject to the usual initial conditions and boundary conditions, but also regularity conditions at the coordinate boundary $r = 0$. Because the Yang-Mills field has two vacuum states, $W = \pm 1$, then we may choose to set $W(0,t) = W_0 = 1$, with $W(\infty,0) = \pm 1$ following from that choice [7]. Specifying the initial conditions involves specifying $W(r,0)$ with $W(0,0) = 1$. The regularity conditions imply $a(0,t) = 1$, $a_r(0,t) = 0$, and $\alpha_r(0,t) = 0$. We have further freedom to specify a boundary condition that has t measuring the proper time of observers at constant r, as $r \to \infty$.

The SU(2) Yang-Mills field, coupled only to gravity, has been studied and displays all behaviour characteristic of critical phenomena [7]. In particular, it displays both type I and type II black hole formation. Figure 4 shows a schematic repesentation of the type of critical behaviour that could occur from a general family of initial data with two parameters p_1 and p_2. Either type

of black hole formation could occur depending on the curve followed in parameter space (p_1, p_2). This provides the encouragement to look for even more interesting behaviour when the SU(2) field is minimally coupled along with a massless scalar field, in particular in the region of parameter space accessible from types I and II collapse.
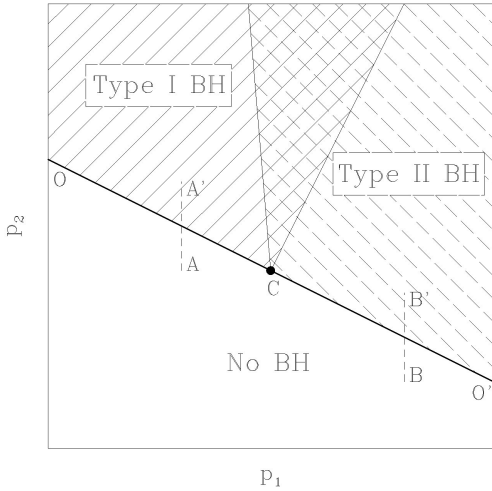

FIG. 4: Schematic representation of type I and type II black hole formation in the collapse of an SU(2) Yang-Mills field. For certain two-parameter families of initial data, there is a critical line OO' separating black hole formation from none, and a critical point C on that line separating the different types of critical behaviour. The overlap of type I and II critical behaviour indicates different behaviour of solutions approaching from the area of parameter space where no black holes form, depending on the direction of approach.

III. DETAILS OF PROPOSED CALCULATION

We aim to solve the system of partial differential equations (9-12) through the use of finite difference approximations. These methods replace the continuum solutions u with a discrete solutions $\hat{u}$. If the solution is given by a system of partial differential equations represented by $Lu = f$, with f some function and L some differential operator, then we aim to solve a discretized system $\hat{L}\hat{u} = \hat{f}$. We take the solutions $\hat{u}$ given on some *uniform* grid in the coordinates r, t, so that $\hat{f}$ may be evaluated exactly at the grid points, and we seek some discretization $\hat{L}$ of L.

A finite difference operator, $\hat{L}$, is a weighted sum of the discretized solution $\hat{u}$. In the one-dimensional single function case we may write this as

$$\hat{L}\hat{u}_i = \ldots + a_{-1}\hat{u}_{i-1} + a_0\hat{u}_i + a_1\hat{u}_{i+1} + \ldots \quad (16)$$

with a_n constants depending on $\hat{L}$. The spacing between the grid points x_n (at which we find u_n) is a constant h. If we assume a Taylor expansion of u about x_i, then after replacing the $\hat{u}_n$ in (16) by the expansion of u evaluated at x_n, and rearranging terms, we get

$$\begin{aligned}
L\hat{u}_i = {}& u\left(\ldots + a_{-1} + a_0 + a_{+1} + \ldots\right) \\
& + u'h\left(\ldots - 2a_{-2} - a_{-1} + a_1 + 2a_2 + \ldots\right) \\
& + u''\frac{h^2}{2}\left(\ldots + 2^2 a_{-2} + a_{-1} + a_1 + 2^2 a_2 + \ldots\right) \\
& + \ldots \quad (17)
\end{aligned}$$

From this, one may make appropriate choices of the a_n in order to obtain the kth order derivative by letting the sum of coefficients in front of u', ... , $u^{(k-1)}$ to be 0, and the sum of coefficients in front of $u^{(k)}$ to be $\frac{k!}{h^k}$. One may furthermore obtain this accurate to the lth order by requiring the sum of coefficients in front of $u^{(k+1)}$, ... , $u^{(k+l)}$ to be 0 as well [15].

Following this procedure, one may find an appropriate finite difference operator $\hat{L}$ for the system, which yields an *algebraic* system of equations over the grid. In general, given our view of an initial value problem, we will be determining the solution on the spatial grid at successive time steps. In most cases, however, the solution at some spatial grid point x_J at time step $n + 1$ will depend not only on the solution up to the previous time step n, but also on other spatial locations at the time step $n + 1$. In order to solve these coupled algebraic equations, one may need to use iterative methods, the choice of which could greatly impact the efficiency of the computation.

The technique of Adaptive Mesh Refinement (AMR) will be considered in order to produce a precise solution where it is needed, without using an unnecessarily fine mesh everywhere. The AMR technique uses a hierarchy of grid coarseness, and in different sections of the spatial domain, evaluates the discrete solution $\hat{u}$ on a grid of a certain coarseness. The coarseness of the grid can be increased for a particular region of the spatial domain if doing so makes a sufficiently small change to the solution, or decreased if further resolution benefits the solution. The coarseness of the grids may be changed throughout the course of the computation, perhaps periodically after a certain number of time steps. This allows the accuracy of a fine grid precisely when and where the evolution demands it. Furthermore, this avoids the complication of choosing appropriate finite difference operators for a non-uniform grid, a considerably more difficult task than for the case of a uniform grid.

In order to detect the formation and mass of black holes, it is convenient to define the mass aspect function $m(r, t)$ by

$$a^2(r, t) = \left(1 - \frac{2m(r, t)}{r}\right)^{-1}. \quad (18)$$

Then if a black hole is formed in our chosen coordinates, the quantity $\frac{2m}{r}$ rapidly asymptotes to 1 at some value of $r = R_{\text{B}}$, the radius of the black hole [6]. Also, the mass of the black hole is given by $M_{\text{B}} = \frac{R_{\text{B}}}{2}$. This allows

convenient detection of black hole formation and investigation of critical behaviour, despite the fact that our choice of coordinates becomes singular when a black hole forms.

IV. RESOURCES LIST

Imposing the condition of spherical symmetry yields a computation far less resource intensive than one even with cylindrical symmetry. Spherical symmetry reduces the problem to a single spatial dimension. This yields a number of grid points, N, on the order of $\frac{L}{h}$, where h is the grid point spacing and L the size of the spatial domain. However, in n spatial dimensions the grid size will be on the order of N^n, meaning there are N^{n-1} times as many grid points to update every time step. Furthermore, imposing spherical symmetry means great simplifications to Einstein's equations, reducing the problem to only two metric components. This puts the bulk of the work into solving the equations of motion for the matter fields. The `vn` cluster at UBC will be used for the majority of the computations. As outlined above, the computational requirements will be rather minimal, and many of the computations may be reasonably performed on a personal computer [9]. In contrast, the fully three-dimensional case is still too resource intensive to be solved to reasonable accuracy [13].

V. PLANNED SCHEDULE

Much of the background theory and numerical methods will be analogous to the case of collapse problems with a single massless scalar field as a matter source. The more complicated nature of the Yang-Mills field, combined with the additional coupling of a massless scalar field, increases the size and complexity of the system of partial differential equations that we are solving. However, the spirit of the computation is the same. With this in mind, we propose the schedule given in table I.

Date	Goal
December	Derivation of equations of motion completed, and choice of coordinates made. Initial, boundary and regularity conditions derived.
Mid-January	Numerical solution to the massless scalar field collapse completed. Choice of numerical scheme made, based on results of massless scalar field collapse.
February	Code for full problem completed.
Late February	Simulations run, and analysis of critical behaviour completed.
Mid-March	Thesis completed, subject to final revisions.

TABLE I: Planned Schedule

Acknowledgments

[1] Abrahams, A. and C. Evans, *Phys. Rev. Let* **70** (1993) 2980

[2] Arnowitt, R., S. Deser and C. Misner. "The Dynamics of General Relativity.", in *Gravitation - an Introduction to Current Research*, L. Witten, ed. New York: Wiley, 1962.

[3] Bardeen, J. and T. Piran, *Phys. Rep.* **96**, 205 (1983)

[4] Brady, P., C. Chambers and S. Goncalves, *Phys. Rev. D* **56**, (1997) 6057

[5] Choptuik, M. Ph.D. Thesis, The University of British Columbia, (1986)

[6] Choptuik, M., *Phys. Rev. Lett.* **70** (1993) 9

[7] Choptuik, M., T. Chmaj and P. Bizon, *Phys. Rev. Lett.* **77**, (1996) 424

[8] Choptuik, M., E. Hirschmann, S. Liebling and F. Pretorius, *Phys. Rev. D* **68** (2003) 044007

[9] Choptuik, M. Personal communication (2006)

[10] D. Christodoulou, *Comm. Math. Phys.* **105**, (1986) 337.

[11] D. Christodoulou, *Commun. Pure Appl. Math.* **44**, (1991) 339.

[12] Gundlach, C., *Physics Reports* **376** (2003) 339

[13] Lehner, L., *Class. Quantum Grav.* **18**, (2001) R25

[14] Misner, C., K. Thorne and J. Wheeler, *Gravitation*, W.H. Freeman, San Francisco, 1973.

[15] Pretorius, F. Ph.D. Thesis, The University of British Columbia, (2002)

[16] Price, R. and J. Pullin, *Phys. Rev. Let.* **75**, (1994) 3297